



CO adsorption and dissociation on iron oxide supported Pt particles

Y.-N. Sun, Z.-H. Qin, M. Lewandowski, S. Shaikhutdinov*, H.-J. Freund

Abteilung Chemische Physik, Fritz-Haber-Institut der Max-Planck-Gesellschaft, Faradayweg 4-6, Berlin 14195, Germany

ARTICLE INFO

Article history:

Received 8 June 2009

Accepted for publication 24 August 2009

Available online 28 August 2009

Keywords:

Platinum

Iron oxides

CO adsorption

CO dissociation

Strong metal support interaction

ABSTRACT

We studied CO adsorption on Pt particles deposited on well-ordered $\text{Fe}_3\text{O}_4(1\ 1\ 1)$ thin films grown on Pt(1 1 1) by temperature programmed desorption (TPD). A highly stepped Pt(1 1 1) surface produced by ion sputtering and annealing at 600 K was studied for comparison. Structural characterization was performed by scanning tunneling microscopy and Auger electron spectroscopy. The TPD spectra revealed that in addition to the desorption peaks at ~ 400 and 480 K, assigned to CO adsorbed on Pt(1 1 1) facets and low-coordination sites respectively, the Pt nanoparticles annealed at 600 K exhibit a desorption state at ~ 270 K. This state is assigned to initial stages of strong metal support interaction resulting in partial Fe–Pt intermixing. On both Pt/ $\text{Fe}_3\text{O}_4(1\ 1\ 1)$ and stepped Pt(1 1 1) surfaces CO is found to dissociate at 500 K. The results suggest that CO dissociation and carbon accumulation occur on the low-coordinated Pt sites.

© 2009 Elsevier B.V. All rights reserved.

1. Introduction

Adsorption of carbon monoxide on platinum surfaces is one of the most explored reactions in surface science (e.g., see [1]). Numerous studies performed on clean Pt single crystal surfaces showed that CO preferentially occupies atop sites on Pt surfaces and also bridge sites at increasing coverage. The binding energy of CO depends on the Pt surface structure. From surfaces with the low Miller indices CO desorbs in a relatively broad signal, between 300 and 550 K, in temperature programmed desorption (TPD) spectra [2–6]. Stepped and kinked Pt surfaces typically exhibit two distinct desorption states, i.e. at ~ 400 and 500 K [6–8], which have been assigned to the (1 1 1)-like terraces and low-coordination sites, respectively. A similar assignment was applied for supported Pt particles [9–12]. For example, Pt particles, deposited at low coverage both on amorphous alumina and $\alpha\text{-Al}_2\text{O}_3(0\ 0\ 0\ 1)$ supports at 300 K, showed a single desorption peak at ~ 510 K, while the larger aggregates revealed an additional desorption state at ~ 400 K [9,10].

It was generally believed that Pt does not appreciably dissociate CO, although controversial results were reported [5–8,13–16]. Somorjai and co-workers first showed that CO dissociation on Pt is, in fact, a surface structure sensitive reaction [13]. Using X-ray photoelectron spectroscopy, they observed carbon deposition upon CO adsorption on the Pt(s)-6(1 1 1) \times (7 1 0) surface. The Pt atoms at steps and kinks were assigned to the sites for CO dissociation. Using field emission microscopy for a Pt single crystal rod, Li and

Vanselow [15] also showed that the kinked areas facilitate CO dissociation. The latter was clearly observed at elevated CO pressures. Using sum frequency generation spectroscopy at 40 Torr of CO and Auger electron spectroscopy (AES) McCrea et al. showed that CO dissociation occurs on Pt(1 1 1), Pt(5 5 7) and Pt(1 0 0) at 673, 548 and 500 K, respectively [17]. The authors suggested that dissociation proceeds via CO-induced surface roughening at high pressures and temperatures, but this mechanism was revisited in the more recent work by Rupprechter et al. [16].

When supported on reducible transition metal oxides such as CeO_2 and TiO_2 , Pt particles exhibit a so-called strong metal support interaction (SMSI) [11,18,19] resulting in a dramatic decrease of CO uptake due to particles' encapsulation by the reduced oxide support at elevated temperatures (typically, above 700 K). We have recently demonstrated that Pt particles supported on well-ordered iron oxide $\text{Fe}_3\text{O}_4(1\ 1\ 1)$ films also undergo the SMSI effect via encapsulation [20,21]. Scanning tunneling microscopy (STM) studies showed that the top facets of the Pt particles annealed at temperatures above 800 K exhibit the structure of a $\text{FeO}(1\ 1\ 1)$ film grown on Pt(1 1 1).

In this work, we studied CO adsorption on Pt particles supported on $\text{Fe}_3\text{O}_4(1\ 1\ 1)$ by TPD, AES, and STM. Perfect and highly stepped Pt(1 1 1) surfaces were used as reference materials. The results indicate that vacuum annealing at 600 K, i.e. before the FeO overgrowth has been observed, causes Fe migration on/into the Pt particles as the initial stage of the SMSI. On both Pt/ $\text{Fe}_3\text{O}_4(1\ 1\ 1)$ and stepped Pt(1 1 1) surfaces CO is found to dissociate at 500 K resulting in carbon deposition. The TPD results suggest that CO dissociation and carbon accumulation occur on the low-coordinated Pt sites.

* Corresponding author. Tel.: +49 030 8413 4114; fax: +49 030 8413 4105.
E-mail address: shamil@fhi-berlin.mpg.de (S. Shaikhutdinov).

2. Experimental

The experiments were performed in two UHV chambers (TPD and STM, base pressure below 3×10^{-10} mbar) equipped with a low energy electron diffraction/Auger electron spectroscopy setup (LEED/AES, from Specs), and a quadrupole mass-spectrometer (QMS, Hiden HAL 301). In the TPD chamber the Pt (1 1 1) crystal (~ 10 mm in diameter, 1.5 mm in thickness, from Mateck) was spot-welded to two parallel Ta wires used for resistive heating and also for cooling by filling a manipulator rod with liquid nitrogen. The temperature was measured by a chromel–alumel thermocouple spot-welded to the backside of the crystal.

In the STM chamber the Pt(1 1 1) crystal, mounted to a Pt sample holder, was heated by electron bombardment from the backside. The temperature was controlled using a chromel–alumel thermocouple spot-welded to the edge of the crystal. In both chambers the crystal temperature was controlled using a feedback control system (Schlichting Phys. Instrum.)

The preparation of thin $\text{Fe}_3\text{O}_4(1\ 1\ 1)$ films on Pt(1 1 1) is described elsewhere [22,23]. Briefly, one monolayer (ML) of Fe is deposited onto clean Pt(1 1 1) at 300 K and subsequently annealed in 10^{-6} mbar O_2 at 1000 K for 2 min to form a $\text{FeO}(1\ 1\ 1)$ monolayer film. Repeated cycles of 5 ML Fe deposition and oxidation results in $\text{Fe}_3\text{O}_4(1\ 1\ 1)$ films as judged by LEED and STM. The average thickness of the films used in this work is about 10 nm.

Iron and Pt (both 99.95%, Goodfellow) were deposited using electron beam assisted evaporators (Focus EFM3). During deposition, the sample was biased with a retarding potential to prevent metal ions from being accelerated towards the sample. Calibration of Pt deposition rate in the TPD chamber was performed with a quartz microbalance.

3. Results and discussion

Fig. 1a and b show typical large-scale STM images of Pt/ $\text{Fe}_3\text{O}_4(1\ 1\ 1)$ surfaces that were annealed in UHV at 600 K for 5 min. The vacuum annealing was performed in order to eliminate structural changes during CO TPD experiments. At sub-monolayer coverage Pt forms two-dimensional islands, while large, well-faceted Pt particles are formed at higher coverage. Although atomic resolution was not achieved on Pt deposits (but on bare support, see [20,21]), it is conceivable that Pt particles grow on a $\text{Fe}_3\text{O}_4(1\ 1\ 1)$ film via the same epitaxial relationships as between the film and the Pt(1 1 1) substrate underneath. The height of the particles seen in Fig. 1a is about 0.5 nm, on average, that roughly corresponds to 2 layers of Pt(1 1 1). At high coverages the particles

grow both in lateral size and height (up to ~ 1 nm) while exposing atomically flat Pt(1 1 1) top facets as shown in Fig. 1b.

Fig. 2a shows CO TPD spectra of a Pt/ $\text{Fe}_3\text{O}_4(1\ 1\ 1)$ surface annealed to 600 K as a function of Pt coverage. The low-temperature signals, i.e. below 200 K, were observed on the pristine films prior to Pt deposition (not shown here). The highest desorption state, found for the clean films, i.e. at ~ 230 K (see also [24]), has been associated with defect sites, which are now decorated by Pt and are, therefore, not visible in the spectra presented. Thus, three desorption peaks, centered at 270, 400 and 480 K, with the coverage-dependent intensity ratios are related to Pt particles. The latter peak is more pronounced at the low Pt coverage, whereas the signals at 400 and 270 K gain intensity with increasing coverage.

On the basis of the literature results [9–12], the desorption states at 400 and 480 K can be explained in terms of CO adsorbed on Pt(1 1 1) facets and low-coordination sites, respectively. To validate this assignment, Fig. 2b depicts a TPD spectrum of CO obtained on the Pt(1 1 1) surface produced by 1 keV Ar^+ ion sputtering at 300 K and subsequent annealing at 600 K for 5 min. This treatment yields a rough surface with a small width of Pt(1 1 1) terraces and a high density of low-coordination sites (step edges and kinks), as illustrated by the STM image in Fig. 1c (see also [25]). Besides the main TPD signal from the Pt(1 1 1) surface (centered at 400 K), an additional peak at ~ 510 K is clearly seen, that is assigned to CO adsorption on the low-coordinated Pt atoms. The absence of the 270 K state on the roughened Pt(1 1 1) surface indicates that this state is intrinsic to the Pt/ $\text{Fe}_3\text{O}_4(1\ 1\ 1)$ surface.

One could, in principle, associate this feature with other than (1 1 1) facets, constituting a particle surface, such as (1 0 0) and, to a lesser extent, (1 1 0) [26]. However, to the best of our knowledge, these two surfaces do not exhibit such a low-temperature desorption peak [27–31]. In fact, the Pt(1 0 0) surface exhibits a desorption peak at higher temperature than that of Pt(1 1 1). Finite size effects are unlikely, too: The particles contain hundreds of Pt atoms, on average, and showed almost bulk behaviour in X-ray photoelectron spectra (not shown). If the 270 K state were the metal/oxide interfacial sites, one would expect to have more of these sites at low Pt coverage where the particles are smaller and the density is higher (see Fig. 1). In fact, Fig. 2a shows that the intensity of the 270 K signal scales with Pt coverage. Bearing in mind that Pt is prone to the SMSI effect with transition metal oxides via encapsulation at elevated temperatures, in particular occurring on the $\text{Fe}_3\text{O}_4(1\ 1\ 1)$ films at ~ 800 K [20,21], we have tentatively linked the 270 K signal to the initial stages of SMSI effects. This interaction could, in principle, result in the support material (Fe and O) migration onto the Pt particles at 600 K.

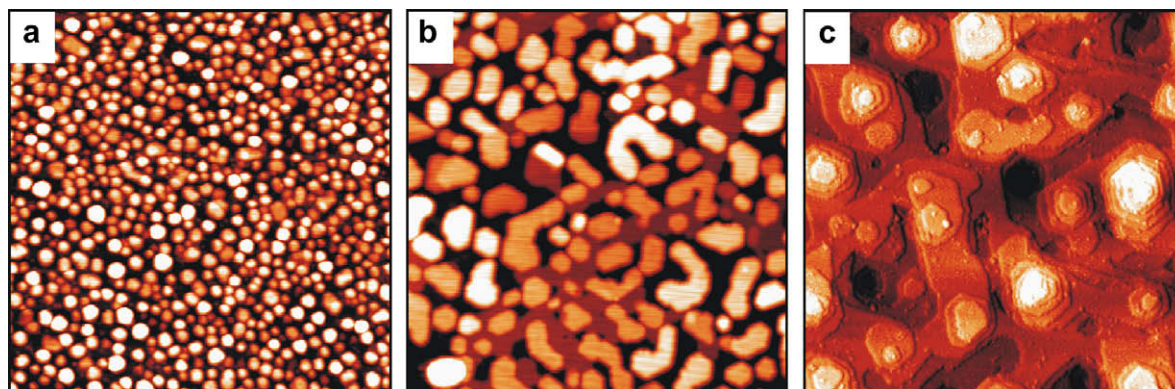


Fig. 1. STM images of the Pt/ $\text{Fe}_3\text{O}_4(1\ 1\ 1)$ surface annealed to 600 K in UHV for 5 min at 0.8 ML Pt (a) and 2.6 ML (b) Pt coverages. Image (c), presented in differentiated contrast, shows a Pt(1 1 1) single crystal surface sputtered by 1 keV Ar^+ ions at 300 K and then annealed to 600 K for 5 min. Image size is 100×100 nm; tunneling bias and current are $V_s = 1.4$ V, $I = 1$ nA (a) 1.4 V and 0.7 nA (b) 0.7 V and 0.4 nA (c).

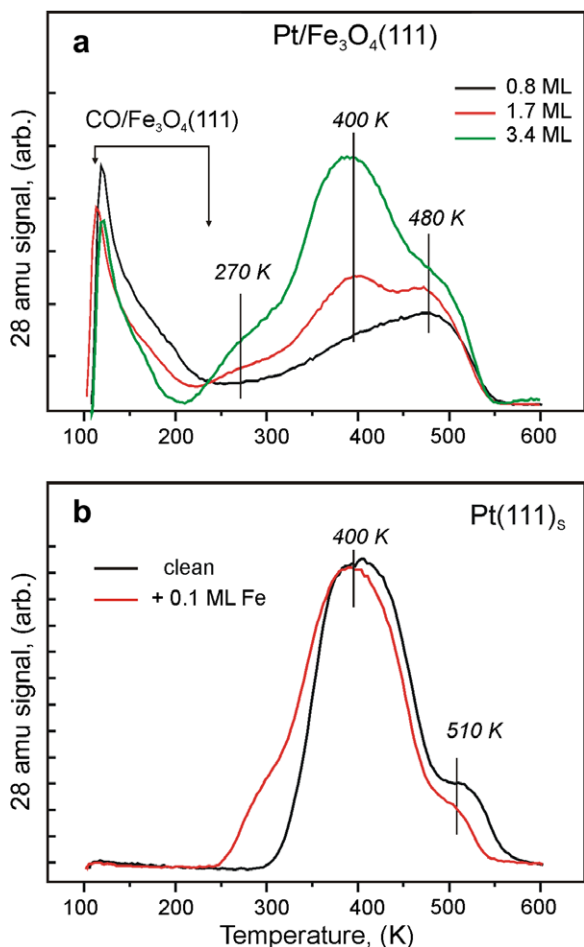


Fig. 2. (a) TPD spectra of CO on Pt/Fe₃O₄(1 1 1) annealed at 600 K for 5 min as a function of Pt coverage as indicated. (b) TPD spectra of CO on the stepped Pt(1 1 1) surface prepared by 1 keV Ar⁺ sputtering at 300 K and annealing at 600 K for 5 min. Subsequently, 0.1 ML of Fe were deposited onto Pt(1 1 1)_s surface and annealed for 5 min at 600 K prior CO adsorption. 7.5 L of CO were dosed at 100 K in each case. The heating rate is 3 K/s.

An O spillover onto Pt seems to be hardly possible since the affinity of Pt for oxygen is obviously lower than that of Fe. Therefore, we first address Fe migration onto Pt. To examine this hypothesis, we studied CO adsorption on 0.1 ML Fe deposited onto the stepped Pt(1 1 1) surface at 300 K and subsequently annealed in UHV at 600 K for 5 min, i.e. as in the case of Pt/Fe₃O₄. For this low Fe coverage one would expect Fe decorating the step edges. However, according to infrared studies [32] and Monte-Carlo simulations [33], the Fe atoms may also migrate into the sub-surface region of Pt at temperatures above ~450 K. Nonetheless, Fig. 2b shows that the intensity of the high temperature peak (~510 K) on the Fe/Pt(1 1 1) surface is reduced by a factor of 2, while the CO capacity of the (1 1 1) terraces is almost unchanged. Interestingly, the new CO desorption state emerges below 300 K, i.e. very similar to that observed on the Pt/Fe₃O₄ surface (see Fig. 2a). Weakening of the CO bond on Pt–Fe surfaces has previously been reported for the Pt-terminated Pt₈₀Fe₂₀(1 1 1)-(2×2) surface, where a main desorption peak is observed at ~340 K [34]. The similar downshift of CO desorption by surface alloying with other metals has also been reported, e.g. on Pt–Sn [35] and Pt–Ce [36] surfaces. Therefore, the results indicate that the 270 K peak observed on the Pt particles originates from Fe migration onto the Pt particles or partial Pt–Fe intermixing upon heating to elevated temperatures.

Fig. 3 shows TPD results for CO adsorbed on 1.7 ML Pt/Fe₃O₄(1 1 1) at 100 K, where also the CO₂ signal (44 amu) was monitored. Two CO₂ desorption peaks are observed at ~150 and ~500 K, which are definitely not due to CO cracking in the mass spectrometer. The signal at 150 K has been detected on pristine Fe₃O₄(1 1 1) films and thus assigned to CO₂ adsorption on the oxide surface from the vacuum background upon cooling the sample to 100 K. The experiments with CO on O-precovered Pt(1 1 1) revealed CO₂ formation in a broad peak between 300 and 400 K (not shown), which is missing in these spectra. Although there is some CO₂ intensity at around 200 and 300 K, which could, in principle, be assigned to CO + O reaction on Pt(1 0 0) facets [31], the signal does not change upon repeating the spectra and most likely originates from the heating wires, etc. and thus can be neglected. Therefore, the results show no evidence for O spillover onto Pt particles.

The most prominent signal at ~500 K must be attributed to the reaction limited desorption of CO₂ that forms on the Pt/Fe₃O₄(1 1 1) interface. The isotopic experiments with C¹⁸O revealed that the O atoms for this reaction come from the iron oxide film as solely the formation of C¹⁶O¹⁸O was observed on the Pt/Fe₃O₄(1 1 1) surface. Since CO on the (1 1 1) facets desorbs at much lower temperatures, CO₂ can only be formed from CO more strongly bound to the sites that are interfacial in nature. This finding further supports the conclusion that the 270 K state cannot be assigned to the metal/oxide interface. In addition, the results show that CO on the interface sites desorbs at the same temperature (i.e. 480 K) as for other low-coordination sites such as edges and corners.

Fig. 3 shows that the CO₂ production at 500 K gradually decreases in repeated CO TPD runs, indicating that oxygen reacted with CO cannot be replenished under these conditions. Interest-

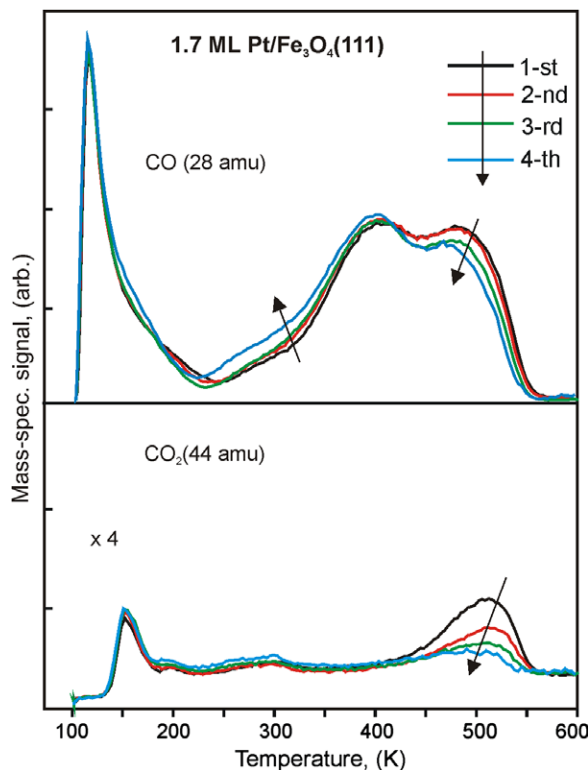


Fig. 3. Repeated TPD spectra of 7.5 L CO adsorbed at 100 K on 1.7 ML Pt/Fe₃O₄(1 1 1). The 28 (CO) and 44 (CO₂) amu signals are shown. The heating rate is 3 K/s.

ingly, the high temperature CO peak also loses intensity. In fact, the CO capacity for this state is reduced even more if one takes into account the amounts of CO that is not desorbed, but consumed to form CO_2 in the previous runs. In principle, this effect could be explained by CO-induced surface restructuring (note, that the surface has been annealed for 5 min at 600 K in UHV prior to TPD studies), site blocking by carbon deposition through CO dissociation (note, however, that the above isotopic experiments showed the Boudouard reaction ($2\text{CO}^{18} \rightarrow \text{CO}_2^{18} + \text{C}$) to be unfavorable), or both. The effects are expected to manifest themselves more strongly at high CO exposures.

Fig. 4a shows CO TPD spectra for 1.7 ML $\text{Pt}/\text{Fe}_3\text{O}_4(111)$ pre-exposed to 1500 L CO ($\sim 10^{-6}$ mbar, 30 min) first at 450 and then at 500 K. It is clear that CO exposure at 450 K essentially causes no change, whereas the exposure at 500 K (i) strongly reduces CO desorption from the high temperature state (i.e. 480 K); (ii) does not appreciably change CO capacity on $\text{Pt}(111)$ terrace sites (at ~ 400 K); and (iii) increases the signal at 100–300 K overlapping with the signal from the support. Very similar results are observed for highly stepped $\text{Pt}(111)_s$ as shown in Fig. 4b. Also for the 0.1 ML $\text{Fe}/\text{Pt}(111)_s$ surface, the CO exposure at 500 K further reduces the signal at ~ 500 K and increases the intensity of the low-temperature shoulder due to carbon deposition (see Fig. 4c). AES analysis revealed carbon formation after experiments at 500 K (see the insets). Meanwhile, the same treatment, applied to the perfect $\text{Pt}(111)$ surface, showed no carbon signal in Auger spectra and no changes in CO TPD (not shown).

Therefore, the results suggest that it is not the Fe–Pt intermixing within the supported Pt particles that is responsible for the CO dissociation at 500 K. In fact, the effect on $\text{Fe}/\text{Pt}(111)_s$ is less pronounced than on the clean $\text{Pt}(111)_s$ surface (cf Fig. 4b and c), most likely due to Fe decorating the low-coordinated Pt surface atoms on which CO dissociation occurs. Indeed, both at 450 and 500 K, the (111) terraces are virtually clean in the 10^{-6} mbar CO pressure used in these experiments, while CO has sufficient residence time on the low-coordination sites to dissociate before desorption. Apparently, the activation energy for CO dissociation is comparable with CO desorption energy on these sites, i.e. about 130 kJ/mol calculated using the Redhead formula [37] and a frequency pre-factor 10^{13} s^{-1} . The carbon left by CO dissociation accumulates on the Pt low-coordinated sites and thus suppresses CO desorption from the high temperature state, i.e. at 480–500 K.

In order to determine whether CO dissociation depends on the Pt particle size, the experiments were performed for different Pt coverages as shown in Fig. 5. For all samples, high CO exposure at 500 K resulted in carbon deposition as shown in the AES spectra presented in the insets. Concomitantly, the 480 K peak is strongly reduced, in particular for the highest Pt coverage studied, while a broad desorption signal at temperatures below 300 K gains intensity and overlaps with the signal of the bare support. (Note that the same exposure to pure $\text{Fe}_3\text{O}_4(111)$ films did not result in new CO desorption states and carbon deposition).

The carbon deposits can be removed by reaction with 10^{-6} mbar O_2 at 500 K. The chemisorbed oxygen left on the Pt surface is in turn removed by CO at 450 K, i.e. at the temperature when no CO dissociation occurs (see Fig. 4). This procedure is similar to that previously used for the $\text{Pd}/\text{Al}_2\text{O}_3/\text{NiAl}(110)$ system [38,39], and practically recovers the original CO TPD spectra and cleanliness of the Pt surfaces as judged by AES.

The results, presented in Figs. 4 and 5, show that the CO capacity for the (111) terrace sites is least affected by carbon deposition (as more clearly observed on the stepped $\text{Pt}(111)$ surface). Therefore, it is plausible that carbon blocks the low-coordinated Pt sites and thus weakens CO bonding to the adjacent terrace sites, ultimately resulting in the low-temperature desorp-

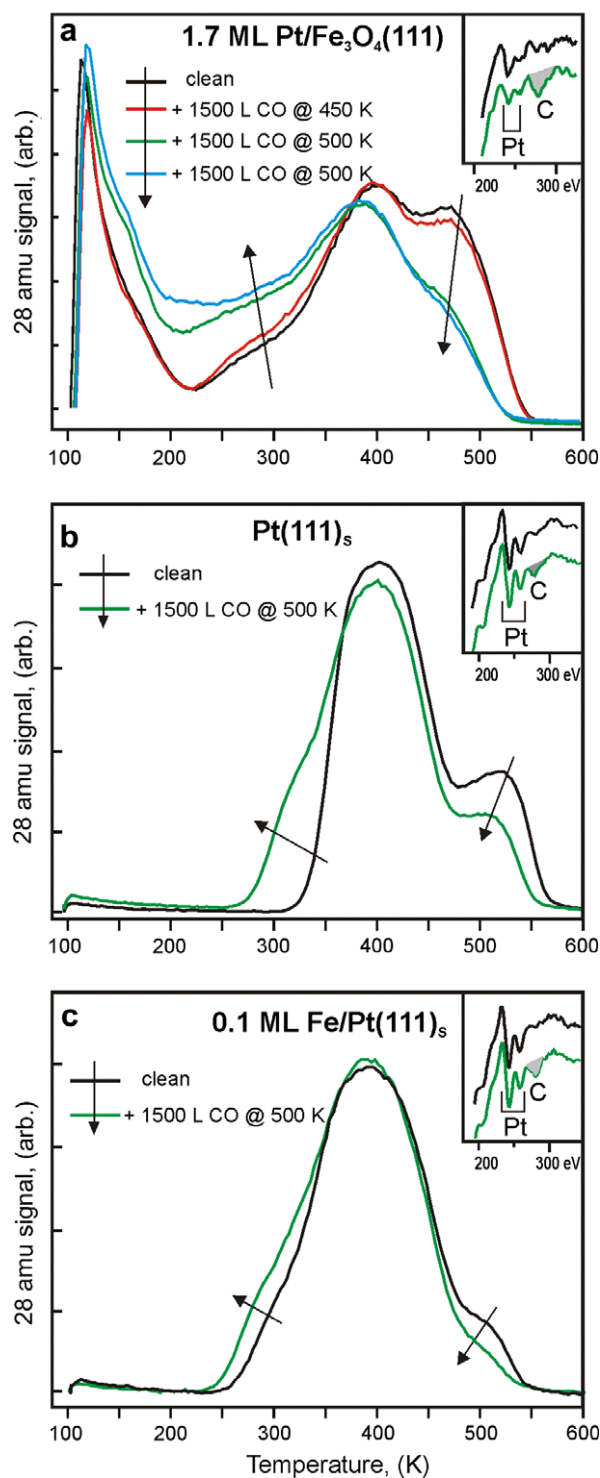


Fig. 4. TPD spectra of CO on (a) $\text{Pt}/\text{Fe}_3\text{O}_4(111)$, (b) stepped $\text{Pt}(111)_s$, and (c) 0.1 ML $\text{Fe}/\text{Pt}(111)_s$ surfaces after high CO exposures as indicated. The heating rate is 3 K/s. The insets show corresponding AES spectra (in the same color code). Formation of carbon upon exposure at 500 K is observed.

tion state below 300 K. Similar changes are observed in experiments with Fe deposition onto the stepped $\text{Pt}(111)$ surface (see Fig. 2), which can be extrapolated to the case of the supported Pt particles. Therefore, we suggest that Fe migrates from the support onto low-coordinated Pt sites upon UHV annealing at 600 K and thus modifies CO adsorption properties in a similar way as carbon.

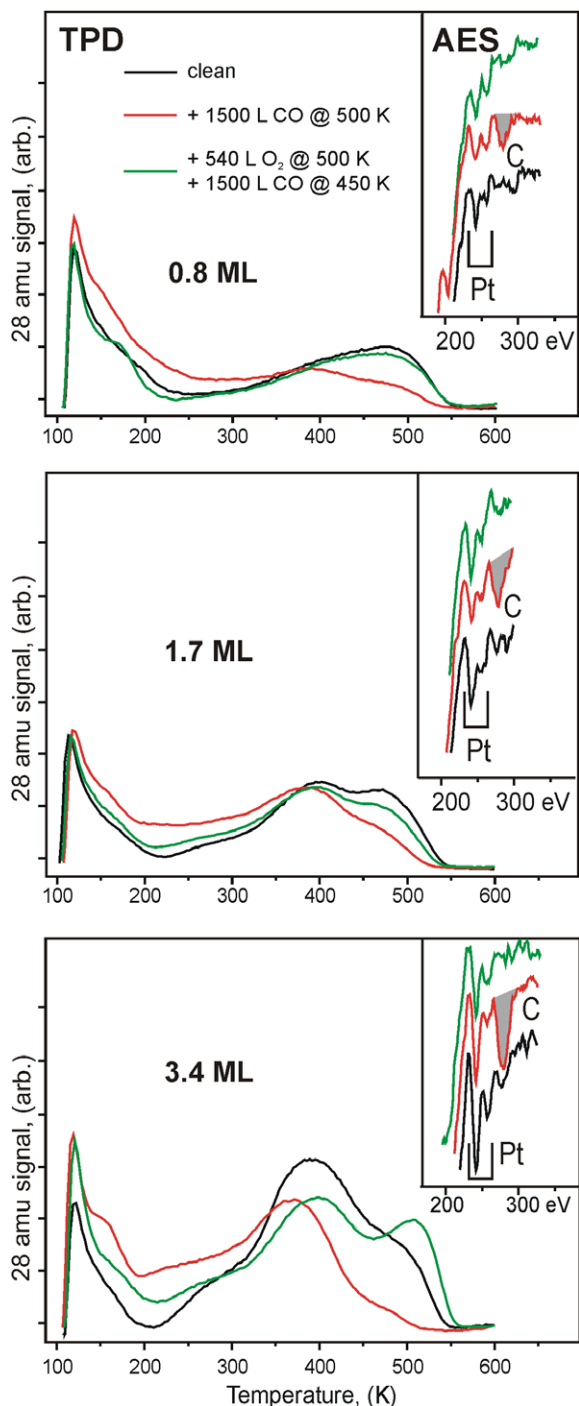


Fig. 5. TPD spectra of CO on Pt/Fe₃O₄(1 1 1) annealed at 600 K for 5 min as a function of Pt coverage as indicated. Then each sample was treated with 1500 L of CO at 500 K. Subsequently, the sample was exposed to 540 L O₂ at 500 K and 1500 L CO at 450 K. 7.5 L of CO were dosed at 100 K in each case. Heating rate is 3 K/s. The corresponding AES spectra are shown in the insets in the same color code.

4. Conclusions

Comparative STM, AES and CO TPD study of Pt/Fe₃O₄(1 1 1), perfect Pt(1 1 1) and highly stepped Pt(1 1 1) surfaces showed that the

Pt nanoparticles annealed at 600 K exhibit a new desorption state at ~270 K. This state is assigned to initial stages of strong metal support interaction resulting in Fe migration onto the Pt particles, although Fe diffusion into the particles at these temperatures cannot be excluded.

Both on Pt/Fe₃O₄(1 1 1) and stepped Pt(1 1 1) surfaces CO is found to dissociate at 500 K resulting in deposition of carbon, supporting the previous literature results on the key role of low-coordinated sites in CO dissociation on Pt. The results also suggest that carbon accumulation occurs on the low-coordinated Pt sites. Carbon deposits can be removed by mild oxidation at 500 K.

Acknowledgements

We thank the Fonds der Chemischen Industrie for financial support.

References

- [1] R. Imbihl, G. Ertl, *Chem. Rev.* 95 (1995) 697.
- [2] R.W. McCabe, L.D. Schmidt, *Surf. Sci.* 66 (1977) 101.
- [3] G. Ertl, M. Neumann, K.M. Streit, *Surf. Sci.* 64 (1977) 393.
- [4] H. Steininger, S. Lehwald, H. Ibach, *Surf. Sci.* 123 (1982) 264.
- [5] D.M. Collins, W.E. Spicer, *Surf. Sci.* 69 (1977) 85.
- [6] H. Hopster, H. Ibach, *Surf. Sci.* 77 (1978) 109.
- [7] B.E. Hayden, K. Kretzschmar, A.M. Bradshaw, R.G. Greenler, *Surf. Sci.* 149 (1985) 394.
- [8] M.R. McClellan, J.L. Gland, F.R. McFeeley, *Surf. Sci.* 112 (1981) 63.
- [9] E.I. Altman, R.J. Gorte, *Surf. Sci.* 172 (1986) 71.
- [10] E.I. Altman, R.J. Gorte, *Surf. Sci.* 195 (1988) 392.
- [11] D.R. Mullins, K.Z. Zhang, *Surf. Sci.* 513 (2002) 163.
- [12] D.L. Doering, H. Poppa, J.T. Dickinson, *J. Vac. Sci. Technol.* 20 (1982) 827.
- [13] Y. Iwasawa, R. Mason, M. Textor, G.A. Somorjai, *Chem. Phys. Lett.* 44 (1976) 468.
- [14] B. Lang, R.W. Joyner, G.A. Somorjai, *Surf. Sci.* 30 (1972) 454.
- [15] X.Q.D. Li, R. Vanselow, *Catal. Lett.* 2 (1989) 113.
- [16] G. Rupprechter, T. Dellwig, H. Unterhalt, H.J. Freund, *J. Phys. Chem. B* 105 (2001) 3797.
- [17] K. McCrea, J.S. Parker, P. Chen, G. Somorjai, *Surf. Sci.* 494 (2001) 238.
- [18] M.A. Vannice, C.C. Twu, *J. Catal.* 82 (1983) 213.
- [19] S.J. Tauster, S.C. Fung, R.L. Garten, *J. Am. Chem. Soc.* 100 (1978) 170.
- [20] Z.H. Qin, M. Lewandowski, Y.N. Sun, S. Shaikhutdinov, H.J. Freund, *J. Phys. Chem. C* 112 (2008) 10209.
- [21] Z.H. Qin, M. Lewandowski, Y.N. Sun, S. Shaikhutdinov, H.J. Freund, *J. Phys.: Condens. Matter* 21 (2009) 134019.
- [22] W. Weiss, W. Ranke, *Prog. Surf. Sci.* 70 (2002) 1.
- [23] W. Weiss, M. Ritter, *Phys. Rev. B* 59 (1999) 5201.
- [24] C. Lemire, R. Meyer, V.E. Henrich, S. Shaikhutdinov, H.J. Freund, *Surf. Sci.* 572 (2004) 103.
- [25] T. Michely, G. Comsa, *Surf. Sci.* 256 (1991) 217.
- [26] K.H. Hansen, T. Worren, S. Stempel, E. Lægsgaard, M. Bäumer, H.J. Freund, F. Besenbacher, I. Stensgaard, *Phys. Rev. Lett.* 83 (1999) 4120.
- [27] H.P. Bonzel, R. Ku, *J. Chem. Phys.* 58 (1973) 4617.
- [28] G. Kneringer, F.P. Netzer, *Surf. Sci.* 49 (1975) 125.
- [29] R.W. McCabe, L.D. Schmidt, *Surf. Sci.* 60 (1976) 85.
- [30] R.K. Sharma, W.A. Brown, D.A. King, *Surf. Sci.* 414 (1998) 68.
- [31] R.B. Shumbera, H.H. Kan, J.F. Weaver, *J. Phys. Chem. C* 112 (2008) 4232.
- [32] T. Wadayama, H. Osano, T. Maeyama, H. Yoshida, K. Murakami, N. Todoroki, S. Oda, *J. Phys. Chem. C* 112 (2008) 8944.
- [33] C. Pint, G. Bozzolo, J.E. Garcés, *Surf. Sci.* 602 (2008) 559.
- [34] A. Ali, M. Abon, P. Beccat, J.C. Bertolini, B. Tardy, *Surf. Sci.* 302 (1994) 121.
- [35] C. Xu, B.E. Koel, *Surf. Sci. Lett.* 304 (1994) L505.
- [36] B. Vermag, M. Juel, S. Raaen, *Phys. Rev. B* 73 (2006) 033407.
- [37] P.A. Redhead, *Vacuum* 12 (1962) 203.
- [38] S. Shaikhutdinov, M. Heemeier, J. Hoffmann, I. Meusel, B. Richter, M. Bäumer, H. Kuhlbeck, J. Libuda, H.J. Freund, R. Oldman, S.D. Jackson, C. Konvicka, M. Schmid, P. Varga, *Surf. Sci.* 501 (2002) 270.
- [39] S. Schauermann, J. Hoffmann, V. Johaneck, J. Hartmann, J. Libuda, *Phys. Chem. Chem. Phys.* 4 (2002) 3909.